J. Phys. Chem. A **1999,** *103,* 9931−9937 **9931**

Theoretical Studies of B_2Li_n ($n = 1-4$)

Gantasala Naga Srinivas,[†] Tracy P. Hamilton,[†] Jerry A. Boatz,[‡] and Koop Lammertsma*,[†,§]

Department of Chemistry, University of Alabama at Birmingham, Birmingham, Alabama 35294,
Air Force Research Laboratory, AFRL/PRSP, 10 East Saturn Blvd, Edwards AFB, CA-93524, and
Department of Chemistry, Vrije Universiteit, De Boelelaan 1083, 1081 HV Amsterdam, The Netherlands

Received: June 23, 1999; In Final Form: September 16, 1999

Structures and energies of the binary B_2Li_n ($n = 1-4$) clusters are predicted with the HF, MP2, and B3LYP methods using the 6-31G(d) basis set, including energy evaluations at G2MP2 and CBS-Q and the larger 6-311+G(2d) basis set for B3LYP. All systems except B_2Li_4 are also computed with the CASSCF method because of spin contamination for several of the open-shell systems. These were followed by energy evaluations with multiconfigurational perturbation theory. The global B_2Li minimum has a C_{2v} triangular form of which the $^2B_1$ state is 13 kcal/mol more stable than the $^2A_1$ state. A bent double Li-bridged structure (C_{2v}) is the global B_2Li_2 minimum with a 2.0 kcal/mol inversion barrier. The global minimum for B_2Li_3 is a triple Li-bridged propellane-like structure (D_{3h}), and for B_2Li_4 it is the quadruple Li-bridged structure (D_{4h}). All these structure have a high degree of ionicity, but in B_2Li_4 stabilization through LiLi interactions also become important. Structural patterns for the isomers of these clusters are examined. Cohesive energies ($B_2Li_n \rightarrow B_2 + Li_n$) and Li and Li_2 elimination energies are analyzed in terms of cluster stabilities.

Introduction

Small boron−lithium clusters are of interest as high-energy additives to cryogenic hydrogen.[1−6] An understanding of the bonding and energetics of these species is therefore important for the design of such fuel additives. Questions about what these clusters look like and how stable they are need to be answered. It is already well-known from the literature that polylithium compounds prefer nonclassical structures that are very different from their common hydrogen analogues.[7−10] For example, $SiLi_4$ prefers a C_{2v} over a T_d geometry.[11] Hyperlithiated compounds with unconventional structures are known, e.g., OLi_4, OLi_6; SLi_6; CLi_x, $x = 6, 8, 10, 12$; FLi_3, FLi_5; $ClLi_3$, $ClLi_5$; PLi_5.[12−17] Lithium carbides and lithiated hydrocarbons are of interest in intercalated lithium−graphite (as solid-state ionic conductors) and for their importance as organolithium reagents in organic synthesis.[18−22] Even the simplest carbon−lithium clusters offer structural surprises. For example, the doubly bridged D_{2h} structure is the most stable C_2Li_2 isomer,[20] while the global C_2Li_4 minimum is a $Li^+C_2^{2-}Li_3^+$ triple ion “salt”.[22] These two examples are illustrative of the differences in bonding between hydrocarbons and their lithium analogues. Despite the use of lithium boride alloys as anode material, very little is known of boron−lithium clusters. This is sharply contrasted by the abundance of information on boranes, which have been scrutinized for their multicenter bonding.[23] This paper explores how substituting hydrogens for lithium atoms will affect this bonding. Previously, we showed for BLi_n ($n = 1-8$) that each boron−lithium cluster has a large cohesive energy and that boron has a maximum coordination number of six lithiums.[24,25] In the present study we report on the binary B_2Li_n ($n = 1-4$) clusters containing two boron atoms.

Computational Methods

The geometries of the B_2Li_n ($n = 1-4$) clusters were optimized at Hartree−Fock (HF) self-consistent field, at Møller−Plesset second-order perturbation (MP2) theory, and at density functional theory (DFT) using Becke’s three-parameter hybrid exchange functional combined with the Lee−Yang−Parr correlation functionals (B3LYP), all using the 6-31G(d) basis set.[10,26,27] These are shown in Figure 1 together with geometrical parameters. The nature of the stationary points was determined by evaluating the second derivatives of the energy (Hessian matrix).[28] More accurate energies were obtained with the G2MP2 and CBS-Q methods.[29,30] The G2MP2, based on MP2/6-31G(d) geometries and energies obtained with the quadratic configuration interaction QCISD(T) method with additional basis set and higher order level corrections, reportedly gives enthalpies of formation to within 2.5 kcal/mol, while the (correlated) complete basis set (CBS) extrapolation method CBS-Q, which also uses MP2/6-31G* geometries, is an alternative also known for its high accuracy. Because of high-spin contamination for some of the B_2Li, B_2Li_2, and B_2Li_3 structures, and since the spin-projected MP2 energies (PMP2) gave little improvement over the unprojected MP2 energies, additional optimizations were carried out with the complete active space (CASSCF) method (see Figure 1) followed by multiconfigurational quasidegenerate second-order perturbation theory (MC-QDPT2) for higher accuracy in the energies.[31] For B_2Li we used an active space consisting of seven electrons distributed over 12 orbitals, denoted as (7,12). For B_2Li_2 it is denoted as (8,10), and for B_2Li_3 it is denoted as (9,9); UHF natural orbitals (occupation numbers between 1.9992 and 0.0002) are used to define the CAS for the B_2Li_3 system, since CASSCF(9,11) encountered convergence problems with MO’s.[32] The effect of a larger basis set (6-311+G(2d)) on the energies was also investigated for the more economical B3LYP method using geometries optimized at B3LYP/6-31G(d). Total and relative energies of the B_2Li_n ($n = 1-4$) isomers are given in Tables

---

[†] University of Alabama at Birmingham.
[‡] Air Force Research Laboratory.
[§] Vrije Universiteit.

10.1021/jp992105y CCC: $18.00

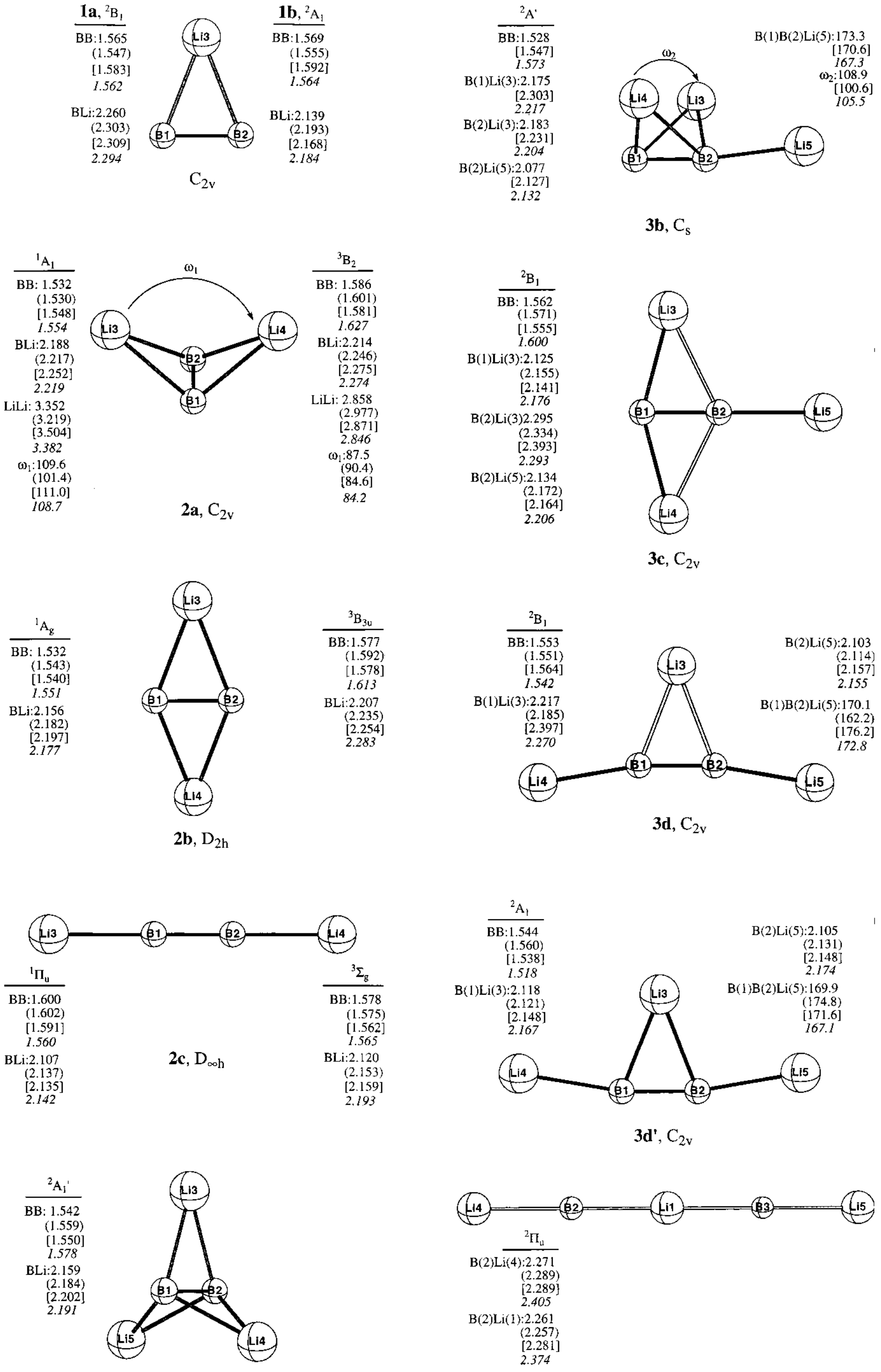

Figure 1. B_2Li_n ($n = 1-4$) structures with geometrical parameters at B3LYP, MP2 (in parentheses), HF (in brackets), and CASSCF (in italics) with the 6-31G(d) basis set.

1−4. All the calculations were carried out with the GAUSSIAN94 and GAMESS program packages.[33,34]

Results and Discussion

Before discussing each B_2Li_n cluster separately, we make some general observations with respect to their geometries. A diversity of structures has been identified with little or no conventional bonding patterns. However, it is evident that in all these structures the two boron atoms are strongly bonded to each other. In fact, the BB bond lengths vary little among these structures, nor are they very sensitive to the different theoretical levels. Thus, the average BB distance is 1.555 ± 0.055 Å at B3LYP. Slightly longer bonds result at both the MP2 (1.562 ± 0.054 Å) and HF (1.558 ± 0.043 Å) levels of theory.

All lithium diborides prefer structures with a maximum of bridging lithiums. Isomers become increasingly less stable with a growing number of terminal lithiums. These terminal BLi bonds have an average BLi distance of 2.135 ± 0.136 Å at B3LYP. Again, slightly longer bonds result at MP2 (2.169 ± 0.120 Å) and HF (2.170 ± 0.119 Å). The bridging BLi bonds are weaker and slightly longer with an average distance of 2.212 ± 0.444 Å at B3LYP. As above, larger distances are found at MP2 (2.241 ± 0.382 Å) and HF (2.272 ± 0.487 Å).

Because no experimental data are yet available for the B_2Li_n clusters, it is important to determine minimum energy structures with some degree of accuracy. Our previous extensive high-level ab initio studies on BLi_n ($n = 1-8$) have shown the need for a careful evaluation of the theoretical methods. For example,

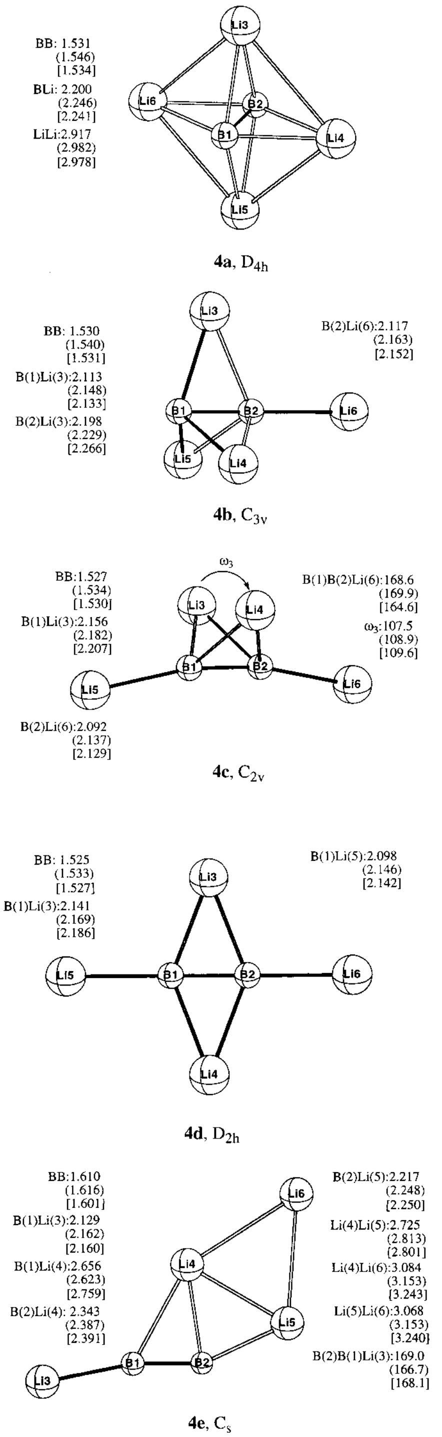

4a, D_{4h}

4b, C_{3v}

4c, C_{2v}

4d, D_{2h}

4e, C_s

Figure 20.

whereas B3LYP/6-31G* performs admirably for the smaller BLi_n clusters ($n = 1-3$) the agreement with MCQDPT2 and G2MP2 for the larger ones ($n = 4-8$) is somewhat less satisfactory. Because these evaluations relied also on boron cohesive energies as well as on Li and Li_2 elimination energies, we perform similar analyses for the clusters of the present study. These data, corrected for zero-point energies, are summarized in Table 5 with the boron cohesive energy defined as the enthalpy for the $B_2Li_n \rightarrow B_2 + Li_n$ reaction.

From the relative and cohesive energies (Tables 1−5) it is evident that the agreement between the theoretical methods varies substantially. As expected, the SCF performance is rather poor and will therefore not be discussed. Except for B_2Li_4, the relative and cohesive energies at MP2/6-31G* compare reasonably well with those at G2MP2, CBS-Q, and MCQDPT2. The difference between B3LYP and these methods is similar. Because it is the most economical one, we will focus on this method to some degree throughout the following sections in which we discuss the geometries and energetics of the various B_2Li_n clusters. Only B3LYP/6-31G* geometrical parameters are used in the discussion unless specifically noted otherwise. We refrain from discussing features of the BLi_n and Li_n fragments that have already been reported upon.[24,25]

TABLE 1: Total (au) and Relative Energies (kcal/mol) for the B_2Li System[a]

str/sym/level	total energy	$\langle S^2\rangle$	relative energy	NIF (cm^{-1})
		1a C_{2v} ($^2B_1$)		
HF	−56.569 28	0.759	0.0	0
MP2	−56.722 42	0.759	0.0	0
B3LYP	−56.991 09	0.753	0.0	0
B3LYP(L)	−57.006 92		0.0	
G2MP2	−56.838 18		0.0	
CBS-Q	−56.834 63		0.0	
CASSCF(7,12)	−56.728 24		0.0	
MCQDPT2	−56.773 16		0.0	
		1b C_{2v} ($^2A_1$)		
HF	−56.547 40	0.863	13.7	0
MP2	−56.701 56	0.857	13.1	0
B3LYP	−56.970 37	0.750	13.0	0
B3LYP(L)	−56.987 72		12.0	
G2MP2	−56.817 81		12.8	
CBS-Q	−56.815 37		12.1	
CASSCF(7,12)	−56.706 79		13.5	
MCQDPT2	−56.753 12		12.6	

[a] Using the 6-31G(d) basis set, except for B3LYP(L), which denotes the use of 6-311+G(2d). NIF indicates the number of imaginary frequencies.

B_2Li. The triangular form is the preferred structure for B_2Li of which the $^2B_1$ state (**1a**) is the global minimum being ca. 13.0 kcal/mol more stable than the $^2A_1$ state (**1b**) at all levels of theory employed. The BB distance of 1.565−1.569 Å is similar for both structures, which is shorter than the 1.618 Å for B_2 ($^3\Sigma_g^-$)[35] but longer than the other lithiated diborides of this study (vide infra). These bond lengths are rather insensitive to the theoretical method employed except for SCF, which generally gives too long bonds. In contrast, the BLi distances differ for the two structures and they vary with the theoretical method. Structure **1b** is the tighter of the two with 0.121 Å shorter BLi distances than the 2.260 Å of **1a**. With CASSCF(7,12), used because of a small degree of spin contamination at HF and MP2, **1a** and **1b** have respectively 0.034 and 0.045 Å longer BLi bond lengths.

Inspection of the molecular orbitals reveals only a small lithium contribution. Essentially, the lithium atom donates its single valence electron to one of the half-filled π_u orbitals of B_2 ($^3\Sigma_g^-$) leading to the two electronic states $^2B_1$ and $^2A_1$. This charge transfer increases the BB bond order and consequently reduces its bond length relative to B_2 ($^3\Sigma_g^-$), which is also reflected in the increased BB vibrational stretching frequency (i.e., 1118 cm^{-1} for B_2Li (**1a**) and 1014 cm^{-1} for B_2 at B3LYP). The natural population analysis (NPA) of **1a** also indicates significant transfer of charge from Li to B_2, which is reflected in the Li charges of $+0.73e$.[36] Not surprisingly, this transfer of charge is even more pronounced in the tighter structure **1b**, i.e., $+0.85e$ for Li. It is evident that the BLi interactions in these structures are very polar.

The stability of B_2Li, and thus the tightness of the BLi interaction, is also evident from its cohesive energy of 63 kcal/mol at G2MP2 (62 kcal/mol at CBS-Q). We note that the

TABLE 2: Total (au) and Relative Energies (kcal/mol) for the B_2Li_2 System[a]

str/sym/level	total energy	$\langle S^2 \rangle$	relative energy	NIF (cm^{-1})
2a C_{2v} ($^1A_1$)				
HF	−64.060 43		0.0	0
MP2	−64.257 28		0.0	0
B3LYP	−64.579 28		0.0	0
B3LYP(L)	−64.596 78		0.0	
G2MP2	−64.375 03		0.0	
CBS-Q	−64.368 68		0.0	
CASSCF(8,10)	−64.211 98		0.0	
MCQDPT2	−64.297 59		0.0	
2a C_{2v} ($^3B_2$)				
HF	−64.081 14	2.251	−13.0	1(149i)
MP2	−64.235 45	2.200	13.7	1(71i)
B3LYP	−64.564 78	2.026	9.1	1(410i)
B3LYP(L)	−64.583 68		8.2	
G2MP2	−64.341 10		21.3	
CBS-Q	−64.339 76		18.1	
CASSCF(8,10)	−64.178 26		21.2	
MCQDPT2	−64.270 51		17.0	
2b D_{2h} (^1A_g)				
HF	−64.046 76		8.6	0
MP2	−64.273 86		−10.4	0
B3LYP	−64.575 07		2.6	1(101i)
B3LYP(L)	−64.593 01		2.4	
G2MP2	−64.371 85		2.0	
CBS-Q	−64.366 01		1.7	
CASSCF(8,10)	−64.207 57		2.8	
MCQDPT2	−64.294 26		2.1	
2b D_{2h} ($^3B_{3u}$)				
HF	−64.091 79	2.034	−19.8	0
MP2	−64.262 00	2.033	−2.9	0
B3LYP	−64.583 99	2.008	−3.4	0
B3LYP(L)	−64.602 05		−3.3	
G2MP2	−64.358 53		10.4	
CBS-Q	−64.356 56		7.6	
CASSCF(8,10)	−64.189 95		13.8	
MCQDPT2	−64.284 74		8.1	
2c $D_{\infty h}$ ($^1\Pi_u$)				
HF	−64.057 24		2.0	0
MP2	−64.207 92		30.9	0
B3LYP	−64.544 99		21.5	0
B3LYP(L)	−64.563 13		21.1	
G2MP2	−64.319 52		34.8	
CBS-Q	−64.314 57		34.0	
CASSCF(8,10)	−64.116 02		60.2	
MCQDPT2	−64.230 55		42.1	
2c $D_{\infty h}$ ($^3\Sigma_g$)				
HF	−64.099 79	2.031	−24.7	0
MP2	−64.237 82	2.029	12.2	0
B3LYP	−64.572 08	2.010	4.5	0
B3LYP(L)	−64.589 05		4.8	
G2MP2	−64.336 08		24.4	
CBS-Q	−64.334 36		21.5	
CASSCF(8,10)	−64.147 49		40.5	
MCQDPT2	−64.253 18		27.9	

[a] See footnote of Table 1.

TABLE 3: Total (au) and Relative Energies (kcal/mol) for the B_2Li_3 System[a]

str/sym/level	total energy	$\langle S^2 \rangle$	relative energy	NIF (cm^{-1})
3a D_{3h} ($^2A_1'$)				
HF	−71.574 61	0.776	0.0	1(720i)
MP2	−71.791 81	0.776	0.0	0
B3LYP	−72.168 44	0.755	0.0	0
B3LYP(L)	−72.187 95		0.0	
G2MP2	−71.893 90		0.0	
CBS-Q	−71.889 41		0.0	
CASSCF(9,9)	−71.670 69		0.0	
MCQDPT2	−71.811 90		0.0	
3b C_s ($^2A'$)				
HF	−71.569 80	1.523	3.0	0
MP2	collapsed to **3a**			
B3LYP	−72.147 23	0.768	13.3	0
B3LYP(L)	−72.166 11		13.7	
CASSCF(9,9)	−71.652 46		11.4	
MCQDPT2	−71.786 53		15.9	
3c C_{2v} ($^2B_1$)				
HF	−71.556 40	0.793	11.4	1(267i)
MP2	−71.748 27	0.793	27.3	1(539i)
B3LYP	−72.136 68	0.757	19.9	0
B3LYP(L)	−72.155 42		20.4	
G2MP2	−71.854 11		25.0	
CBS-Q	−71.850 19		24.6	
CASSCF(9,9)	−71.637 01		21.1	
MCQDPT2	−71.770 47		25.9	
3d C_{2v} ($^2B_1$)				
HF	−71.559 49	1.337	9.5	1(118i)
MP2	−71.743 10	0.820	30.6	0
B3LYP	−72.135 96	0.755	20.4	0
B3LYP(L)	−72.153 65		21.5	
G2MP2	−71.851 57		22.8	
CBS-Q	−71.847 67		22.4	
CASSCF(9,9)	−71.615 71		34.5	
MCQDPT2	−71.759 24		33.0	
3d′ C_{2v} ($^2A_1$)				
HF	−71.542 49	0.948	20.2	0
MP2	−71.728 94	0.884	39.5	0
B3LYP	−72.121 69	0.769	29.3	0
B3LYP(L)	−72.141 87		28.9	
CASSCF(9,9)	−71.600 68		43.9	
MCQDPT2	−71.753 34		36.7	
3e $D_{\infty h}$ ($^2\Pi_u$)				
HF	−71.401 03	0.767	108.9	1(43i)
MP2	−71.546 18	0.767	154.1	0
B3LYP	−71.969 20	0.755	125.0	0
B3LYP(L)	−71.981 09		129.8	
G2MP2	−71.671 62		139.5	
CBS-Q	−71.664 19		141.3	
CASSCF(9,9)	−71.438 83		145.5	
MCQDPT2	−71.538 29		171.7	

[a] See footnote of Table 1.

cohesion energy of 56.3 kcal/mol at B3LYP is slightly less, while the much smaller energies at MP2 and HF for this dissociation of Li indicate the inadequacy of these methods for this system.

B_2Li_2. Three stationary points were characterized on each of the singlet and triplet surfaces. The global minimum at the higher levels of theory is the singlet $^1A_1$ structure **2a**, whereas MP2 and B3LYP prefer instead the ^1A_g and $^3B_{3u}$ states of planar **2b**, respectively. Structure **2a** has a puckering angle of ca. 110°. Inversion via planar **2b** requires only 2.6 kcal/mol (at B3LYP), indicating the butterfly structure to be highly flexible. G2MP2 gives a similar inversion barrier (2.0 kcal/mol) as do CBS-Q, CASSCF, and MCQDPT2, but MP2 favors **2b** instead by as much as 10.4 kcal/mol. On becoming planar, the 1.532 Å BB bond length does not alter, even though the BLi distances decrease with 0.03 Å as a result of stronger ionic interactions. The NPA charges on Li(+) and B(−) are larger for **2b** (0.85*e*) than for **2a** (0.75*e*). Apparently, the second Li atom donates its valence electron to the singly occupied π orbital of B_2Li. This increases the charges and the BB bond order (which is reflected in 0.07 Å shorter BLi distances and a 0.03 Å shorter BB bond length, respectively), culminating in a tighter packed structure of high ionic character. This increased ionicity of **2a**, compared to B_2Li, is supported by the noted NPA charges. Its cohesive energy ($B_2Li_2 \rightarrow B_2 + Li_2$) amounts to a large 102 kcal/mol at G2MP2 and CBS-Q (and 6 kcal/mol less at B3LYP). Its 66

TABLE 4: Total (au) and Relative Energies (kcal/mol) for the B_2Li_4 System[a]

str/sym/level	total energy	relative energy	NIF (cm^{-1})
4a D_{4h}			
HF	−79.041 30	0.0	0
MP2	−79.296 22	0.0	0
B3LYP	−79.727 47	0.0	0
B3LYP(L)	−79.749 95	0.0	
G2MP2	−79.402 81	0.0	
CBS-Q	−79.394 15	0.0	
4b C_{3v}			
HF	−79.042 87	−1.0	0
MP2	−79.290 98	3.3	0
B3LYP	−79.724 34	2.0	0
B3LYP(L)	−79.744 89	3.2	
G2MP2	−79.398 23	2.9	
CBS-Q	−79.390 86	2.1	
4c C_{2v}			
HF	−79.035 37	3.7	0
MP2	−79.277 91	11.5	0
B3LYP	−79.714 78	8.0	0
B3LYP(L)	−79.734 35	9.8	
G2MP2	−79.385 52	10.8	
CBS-Q	−79.377 68	10.3	
4d D_{2h}			
HF	−79.031 44	6.2	1(66i)
MP2	−79.274 43	13.7	1(49i)
B3LYP	−79.711 59	10.0	1(62i)
B3LYP(L)	−79.731 69	11.5	
G2MP2	−79.382 35	12.8	
CBS-Q	−79.375 18	11.9	
4e C_s			
HF	−78.981 49	37.5	0
MP2	−79.156 91	87.4	0
B3LYP	−79.617 57	69.0	0
B3LYP(L)	−79.634 26	72.6	
G2MP2	−79.285 19	73.8	
CBS-Q	−79.276 43	73.9	

[a] See footnote of Table 1.

kcal/mol endothermicity (G2MP2, 60 kcal/mol at B3LYP) for Li elimination is even slightly more (by 3 kcal/mol) than that for B_2Li ($^2B_1$).

On the triplet surface, **2a** ($^3B_2$ state) has a tetrahedral form with a puckering angle of less than 90° and a LiLi distance of only 2.858 Å (B3LYP). This transition structure is 17 kcal/mol less stable than the $^1A_1$ singlet at MCQDPT2. On the other hand, the $^3B_{3u}$ state of rhombic **2b** is a local minimum and only 8.4 kcal/mol (G2MP2, 5.0 kcal/mol at CBS-Q) less stable than the singlet ^1A_g state. We note that the energy differences for these triplet structures are only consistent at the higher levels of theory.

The linear $^1\Pi_u$ state isomer **2c** is a minimum energy structure with a longer BB distance than in **2a** ($^1A_1$) and **2b** (^1A_g). This suggests that in **2c** the Li atom does not donate its valence electron to the Π_u orbitals of B_2 as effectively as in **2a** and **2b**, where the Li atoms are bridging rather than terminal. This notion is also supported by the NPA charges in Table S1 in Supporting Information. Structure **2c** is significantly less stable than the butterfly form **2a**. The energy difference depends strongly on the theoretical method employed and ranges, for example, from 21.5 to 34.8 to 42.1 kcal/mol at B3LYP, G2MP2, and MCQDPT2, respectively. Because of the need for a multiconfigurational approach in these “electron-deficient” linear systems, we consider the energy obtained with multiconfigurational quasidegenerate perturbation theory to be the most accurate. The energy difference of the corresponding $^3\Sigma_g$ state isomer of **2c** (also a minimum) with **2a** varies less with the more sophisticated theories (i.e., 24.4 and 27.9 kcal/mol for G2MP2 and MCQDPT2) but is surprisingly small at B3LYP (4.5 kcal/mol) and large at CASSCF(7,10) (40.5 kcal/mol). The triplet structure is more stable than the singlet form with an energy difference of 14.2 kcal/mol at MCQDPT2.

B_2Li_3. Six minima were identified on the B3LYP hypersurface of doublet B_2Li_3, of which five are also stationary points at MP2. These structures extend the features already seen for the smaller homologues. The global minimum is the B_2 triple Li-bridged propellane structure **3a**. This structure is very similar to the butterfly B_2Li_2 structure **2a** but capped with another Li atom. Its BB bond length of 1.542 Å (B3LYP) is between those of singlet and triplet **2a**, respectively, but its 2.159 Å BLi distance is slightly shorter. The NPA charge on the lithiums is $+0.77e$ each, just as for **2a**. Evidently, all three Li atoms donate their valence electrons to the B_2 ($^3\Sigma_g^-$) unit to occupy its σ_g and two π_u orbitals; the BB distance in B_2^{3-} ($^2\Sigma_g$) is 1.630 Å (B3LYP). The Li dissociation energy for **3a** of 55 kcal/mol at G2MP2 and CBS-Q, though, is 10 kcal/mol less than that for **2a**, which suggests that the exothermicity is reduced on binding a third Li atom to B_2. Because of the LiLi bonding in Li_n, this reduced bonding of the third Li atom is not reflected in the B_2 cohesive energies, which are 145, 102, and 63 kcal/mol at G2MP2 for B_2Li_3, B_2Li_2, and B_2Li, respectively, or ca. 42 kcal/mol per *added* Li atom; the CBS-Q data are similar. Interestingly, B3LYP gives Li dissociation energies of ca. 60 kcal/mol for both **3a** and **2a** and a cohesive energy for **3a** identical to that from G2MP2 (145 kcal/mol). Binding energies at both the HF and MP2 levels of theory are less satisfactory.

Structure **3b** can be viewed as resulting from a Li side-on addition to the butterfly structure **2a**, while **3c** represents its planar form. This planarization requires 6.6 kcal/mol at B3LYP

TABLE 5: B_2 Cohesive Energies and Li and Li_2 Dissociation Energies (in kcal/mol)

reaction	HF[a]	MP2[a]	B3LYP[a]	B3LYP(L)[b]	G2MP2	CBS-Q
B_2 Cohesion						
$B_2Li \rightarrow B_2 + Li$	38.2	44.8	56.3	58.5	63.0	62.1
$B_2Li_2 \rightarrow B_2 + Li_2$	72.0	94.4	96.0	98.4	102.3	102.2
$B_2Li_3 \rightarrow B_2 + Li_3$	114.3	152.2	145.5	148.1	144.6	142.7
$B_2Li_4 \rightarrow B_2 + Li_4$	130.2	173.1	163.0	166.7	159.7	160.6
Li Dissociation						
$B_2Li_2 \rightarrow B_2Li + Li$	36.1	63.4	59.5	60.3	65.7	64.0
$B_2Li_3 \rightarrow B_2Li_2 + Li$	51.2	64.4	60.6	61.6	54.4	55.7
$B_2Li_4 \rightarrow B_2Li_3 + Li$	20.5	44.2	41.4	43.1	48.1	45.6
Li_2 Dissociation						
$B_2Li_3 \rightarrow B_2Li + Li_2$	85.1	113.9	100.3	101.5	93.7	95.8
$B_2Li_4 \rightarrow B_2Li_2 + Li_2$	69.5	94.7	82.2	84.3	76.2	77.4

[a] Using the 6-31G(d) basis set and inclusion of zero-point energy (ZPE) corrections. The MP2 values that involve B_2Li_3 use HF-ZPE corrections. [b] Using the 6-311+G(2d) basis set and B3LYP/6-31G(d) ZPE corrections.

and 10 kcal/mol at MCQDPT2. Interestingly, B3LYP characterizes both structures as minima, while **3b** could not be obtained at MP2. Double-Li-bridged **3b** is less stable than the triple-bridged form by 13.3 kcal/mol at B3LYP (15.9 kcal/mol at MCQDPT2).

The two single-Li-bridged structures **3d** ($^2B_1$ state) and **3d′** ($^2A_1$ state) differ mainly in the tilting angle of their terminal lithium atoms but also have slightly different BB bond lengths and BLi bridging distances. The energy difference between the two isomers amounts to 3.7 kcal/mol at MCQDPT2 (8.9 kcal/mol at B3LYP) of which **3d** is 33 kcal/mol (20 kcal/mol at B3LYP) less stable than the global minimum. From the presence of significant spin contamination we infer that multiconfigurational quasidegenerate perturbation theory gives the more accurate energies.

Structure **3e** represents a Li insertion into the BB bond, separating the boron atoms, and is clearly a high-energy isomer but nonetheless is a minimum at the MP2 and B3LYP levels. It is merely included in this study to illustrate that Li can fulfill a coordinating role in the formation of B_xLi_y clusters from Li and B atoms.

B_2Li_4. The bonding patterns found in the smaller binary B_2Li_n clusters are also present and even extended in B_2Li_4. Four minima and a transition structure were identified. Surprisingly, the global minimum is structure **4a**, which has its 1.531 Å B−B bond bridged by four Li atoms. Each boron is pentacoordinated and has an inverted geometry. Because **4a** and propellane **3a** have similar BB bond lengths, it appears that the fourth lithium does not influence the BB bond strength. The NPA charge on the lithiums of $+0.59e$ each is $+0.18e$ less than in **3a**, while the charge on the B_2 fragment remains at ca. $-2.35e$. Thus, the interaction between the lithiums in **4a** is strongly enhanced, which also agrees with the LiLi distances of 2.971 Å. Similar short distances were found for higher coordinated BLi_n ($n = 4-8$) structures. The cohesive energy of ca. 160 kcal/mol (G2MP2, CBS-Q) translates into 40 kcal/mol per lithium, or 8 kcal/mol less than the per lithium energy for **3a**, which infers a different bonding stabilization in the four-Li-bridged structure. Also the Li and Li_2 dissociation energies of the B_2Li_4 global minimum are smaller than for **3a**.

Structure **4b** resembles **3a** but has an extra Li added side-on. This terminal BLi bond distorts the propellane structure only slightly and reduces the charge of the bridging lithiums to $+0.63e$. Its energy difference with **4a** is only 2.9 kcal/mol at G2MP2 with similar values at the other correlated levels. Evidently, the energy surface for binding the fourth lithium is rather soft, and B_2Li_4 should therefore be a rather flexible system.

Isomer **4c** with the added terminal BLi bond extends the butterfly structures of **3b** and **2a**. Their structural properties are similar except that the terminal BLi bonds in **4c** are tilted downward. Inversion via **4d** (a transition structure) requires only 1.6−2.0 kcal/mol, depending on the theoretical method employed, again illustrating the flexible nature of B_2Li_4. The energy difference of **4c** compared to the global minimum is 10.8 at G2MP2 and slightly less with the other methods.

Even though **4e** seems at first sight an unusual structure, it represents a B_2^{2-} dianion complexed with Li^+ and Li_3^+ cations at opposite sides. The terminal Li has indeed, as expected, an NPA charge of $+0.74e$, but the side-complexed triangular Li_3^+ is strongly polarized with, in fact, a negative charge of $-0.40e$ on the distal Li. Interestingly, the carbon analogue of this structure is among the two most stable C_2Li_4 isomers[22] and has also been formulated as a $Li^+C_2^{2-}Li_3^+$ acetylene triple ion "salt". Diboride **4e** is, however, by far the least stable of the B_2Li_4 isomers.

Conclusions

This computational study of the structural and energetic details of small binary B/Li clusters reveals several characteristics, some of which are unexpected. The structural diversity of these clusters is large and differs from those of both Li/C clusters and diboranes. The most salient features are the following. (1) All B_2Li_n ($n = 1-4$) structures contain a B_2 unit with a short BB bond. (2) Bridging of this B_2 unit by lithiums is preferred for all B_2Li_n ($n = 1-4$) systems including the four Li-bridged B_2Li_4 structure. (3) All display a high degree of ionicity except for the B_2Li_4 structure in which case stabilization also occurs through LiLi interactions. (4) As a result, all structures are rather flexible. (5) B3LYP/6-31G(d) performs rather well in calculating geometries and their relative energies. Use of the extended 6-311+G(2d) basis set has little influence on the relative energies and on neither the B_2 cohesive energies nor the Li and Li_2 dissociation energies. (6) These dissociation energies and even more importantly the relative energies of the isomeric structures are less than satisfactory with HF and MP2/6-31G(d). (7) G2MP2, CBS-Q, and MCQDPT2 perform equally well for most systems. (8) The B_2 cohesive energy tapers off when the fourth lithium is added.

Acknowledgment. This work was supported by the Air Force Office of Scientific Research (Grant F49620-96-1-0450). Several enlightening discussions with Dr. Michael W. Schmidt are gratefully acknowledged.

Supporting Information Available: Tables of NPA charges and harmonic vibrational frequencies. This material is available free of charge via the Internet at http://pubs.acs.org.

References and Notes

(1) Kaufman, J. J.; Sachs, L. M. *J. Chem. Phys.* **1970**, *52*, 645.

(2) Cade, P. E.; Huo, W. M. *At. Data Nucl. Data Tables* **1975**, *15*, 1.

(3) Zhu, Z. H.; Murrell, J. N. *Chem. Phys. Lett.* **1982**, *88*, 262.

(4) Knowles, D. B.; Murrell, J. N. *J. Mol. Struct.: THEOCHEM* **1986**, *135*, 169.

(5) Saxon, R. P. Theoretical Studies of Boron Compounds. *Proceedings of the High Energy Density Matter*, Woods Hole, MA, 1992.

(6) Sheehy, J. A. Spectroscopy of Lithium Boride, A candidate HEDM Species. *Proceedings of the High Energy Density Matter*, Woods Hole, MA, 1995.

(7) Schleyer, P. v. R. *Pure Appl. Chem.* **1983**, *55*, 355; **1984**, *56*, 151.

(8) Maercker, A.; Thies, M. *Top. Curr. Chem.* **1987**, *138*, 1.

(9) Ritchie, J. P.; Bachrach, S. M. *J. Am. Chem. Soc.* **1987**, *109*, 5909.

(10) Hehre, W.; Radom, L.; Schleyer, P. v. R.; Pople, J. A. *Ab Initio Molecular Orbital Theory*; Wiley: New York, 1986.

(11) Schleyer, P. v. R.; Reed, A. E. *J. Am. Chem. Soc.* **1988**, *110*, 4453.

(12) Gillespie, R. J.; Hargittai, I. *The VSEPR Model of Molecular Geometry*; Allyn and Bacon: Boston, 1991.

(13) Schleyer, P. v. R.; Wurthwein, E.-U.; Pople, J. A. *J. Am. Chem. Soc.* **1982**, *104*, 5839.

(14) Ivanic, J.; Marsden, C. J.; Hassett, D. M. *J. Chem. Soc., Chem. Commun.* **1993**, 822.

(15) Schleyer, P. v. R.; Wurthwein, E.-U.; Kaufmann, E.; Clark, T.; Pople, J. A. *J. Am. Chem. Soc.* **1983**, *105*, 5930.

(16) Ivanic, J.; Marsden, C. J. *J. Am. Chem. Soc.* **1993**, *115*, 7503.

(17) Marsden, C. J. *J. Chem. Soc., Chem. Commun.* **1989**, 1356.

(18) Fan, Q.; Pfeiffer, G. V. *Chem. Phys. Lett.* **1989**, *162*, 479.

(19) Ivanic, J.; Marsden, C. J. *Organometallics* **1994**, *13*, 5141.

(20) Schleyer, P. v. R. *J. Phys. Chem.* **1990**, *94*, 5560.

(21) Kos, A.; Poppinger, D.; Schleyer, P. v. R.; Thiel, W. *Tetrahedron Lett.* **1980**, *21*, 2151.

(22) Dorigo, A. E.; van Eikema Hommes, N. J. R.; Krog-Jesperson, K.; Schleyer, P. v. R. *Angew. Chem., Int. Ed. Engl.* **1992**, *31*, 1602.

(23) Cotton, F. A.; Wilkinson, G. *Advanced Inorganic Chemistry*; Interscience: New York, 1972.

(24) Nguyen, K. A.; Lammertsma, K. *J. Phys. Chem. A* **1998**, *102*, 1608.

(25) Nguyen, K. A.; Srinivas, G. N.; Hamilton, T. P.; Lammertsma, K. *J. Phys. Chem. A* **1999**, *103*, 710. Meden, A.; Mavri, J.; Bele, M.; Pejovnik, S. *J. Phys. Chem.* **1995**, *99*, 4252.

(26) Hehre, W. J.; Ditchfield, R.; Pople, J. A. *J. Chem. Phys.* **1972**, *56*, 2257. Møller, C.; Plesset, M. S. *Phys. Rev.* **1934**, *46*, 618.

(27) Becke, A. D. *J. Chem. Phys.* **1993**, *98*, 5648. Becke, A. D. *Phys. Rev. A* **1988**, *38*, 3098. Lee, C.; Yang, W.; Parr, R. G. *Phys. Rev. B* **1988**, *37*, 785. Vosko, S. H.; Wilk, L.; Nusair, M. *Can. J. Phys.* **1980**, *58*, 1200.

(28) Pople, J. A.; Raghavachari, K.; Schlegel, H. B.; Binkley, J. S. *Int. J. Quantum Chem. Symp.* **1979**, *13*, 255.

(29) Curtiss, L. A.; Raghavachari, K.; Pople, J. A. *J. Chem. Phys.* **1993**, *98*, 1293. Curtiss, L. A.; Raghavachari, K.; Trucks, G. W.; Pople, J. A. *J. Chem. Phys.* **1991**, *94*, 7221.

(30) Ochterski, J. W.; Petersson, G. A.; Montgomery, J. A., Jr. *J. Chem. Phys.* **1996**, *104*, 2598. Ochterski, J. W.; Petersson, G. A.; Wiberg, K. B. *J. Am. Chem. Soc.* **1995**, *117*, 11299.

(31) Nakano, H. *J. Chem. Phys.* **1993**, *99*, 7983.

(32) Pulay, P.; Hamilton, T. P. *J. Chem. Phys.* **1988**, *88*, 4926.

(33) Frisch, M. J.; Trucks, G. W.; Schlegel, H. B.; Gill, P. M. W.; Johnson, B. G.; Robb, M. A.; Cheeseman, J. R.; Keith, T.; Petersson, G. A.; Montgomery, J. A.; Raghavachari, K.; Al-Laham, M. A.; Zakrzewski, V. G.; Ortiz, J. V.; Foresman, J. B.; Cioslowski, J.; Stefanov, B. B.; Nanayakkara, A.; Challacombe, M.; Peng, C. Y.; Ayala, P. Y.; Chen, W.; Wong, M. W.; Andres, J. L.; Replogle, E. S.; Gomperts, R.; Martin, R. L.; Fox, D. J.; Binkley, J. S.; Defrees, D. J.; Baker, J.; Stewart, J. P.; Head-Gordon, M.; Gonzalez, C.; Pople, J. A. *GAUSSIAN 94*, revision E.2; Gaussian, Inc.: Pittsburgh, PA, 1995.

(34) Schmidt, M. W.; Baldridge, K. K.; Boatz, J. A.; Elbert, S. T.; Gordon, M. S.; Jensen, J. J.; Koseki, S.; Matsunaga, M.; Nguyen, K. A.; Su, S.; Windus, T. L.; Dupuis, M.; Montgomery, J. A. *J. Comput. Chem.* **1993**, *14*, 1347.

(35) Boldyrev, A. I.; Gonzales, N.; Simons, J. *J. Phys. Chem.* **1994**, *98*, 9931.

(36) Reed, A. E.; Curtiss, L. A.; Weinhold, F. *Chem. Rev.* **1988**, *88*, 899.